Institute of Physics Publishing Journal of Physics: Conference Series **54** (2006) 399–405
doi:10.1088/1742-6596/54/1/063 Galaxy Center Workshop

Infrared/X-ray intensity variations and the color of Sgr A*

S D Hornstein[1], K Matthews[2], A M Ghez[1,3], J R Lu[1], M Morris[1], E E Becklin[1], F K Baganoff[4] and M Rafelski[1]

[1] Department of Physics and Astronomy, University of California, Los Angeles, CA 90095-1547, USA
[2] Caltech Optical Observatories, California Institute of Technology, MS 320-47, Pasadena, CA 91125, USA
[3] Institute for Geophysics and Planetary Physics, University of California, Los Angeles, CA 90095-1565, USA
[4] Kavli Institute for Astrophysics and Space Research, Massachusetts Institute of Technology, Cambridge, MA 02139-4307, USA

E-mail: seth@astro.ucla.edu

Abstract. We report the first time-series measurements of Sgr A*-IR's broadband infrared color. Using the newly commissioned laser guide star adaptive optics (LGS AO) system on the Keck II telescope, we imaged Sgr A*-IR in the broadband filters H (1.6 μm), K' (2.1 μm), and L' (3.8 μm) every 3 minutes over the course of 120 minutes, during which time the Chandra X-ray Observatory was also monitoring the Galactic center. Complementary measurements of Sgr A*'s L'- and M_s (4.7 μm)-band flux densities were obtained on a separate night with the natural guide star AO system. During our observations, Sgr A*-IR's flux density showed a wide range of values (2 to 12 mJy at 2.1 μm), which are associated with at least 4 peaks in the infrared emission and are among its highest infrared flux density measurements. However, all our near-infrared color measurements are consistent with a constant spectral slope of α = -0.9 $\pm$ 0.2 ($F_\nu \propto \nu^\alpha$), independent of intensity, wavelength, time, or outburst. Assuming that the infrared wavelengths probe synchrotron emission, we interpret the lack of variation in the infrared spectral index as an indication that the acceleration mechanism leaves the distribution of the bulk of the electrons responsible for the infrared emission unchanged. During our coordinated infrared observations, no elevated X-ray emission was detected. While the less frequent X-ray outbursts have shown correlated emission in previous studies, the lack of X-ray variation during the significant infrared variations reported here indicates that one may not be able to connect the infrared and X-ray emission to the *same* electrons. We suggest that while the acceleration mechanism leaves the bulk of the electron energy distribution unchanged, it generates a variable high-energy tail. It is this high-energy tail that gives rise to the less frequent X-ray outbursts.

1. Introduction

Since its discovery, the compact source at the center of our Milky Way Galaxy [1], now associated with a 3.7×10^6 $M_\odot$ supermassive black hole [2, 3], has perplexed scientists with its remarkably low luminosity of only 10^{36} erg s^{-1} or, equivalently, 10^{-9} L_{Edd}. The recent detection of variable emission from Sagittarius (Sgr) A* at wavelengths from radio [4, 5, 6] to X-ray [7, 8, 9] has offered a new view into the central engine of our Galaxy and provides possible clues to its behavior. Models attempting to explain the cause of this emission have yet to converge on a physical

cause for the emission but generally rely on a highly-energetic population of electrons producing synchrotron emission at radio and infrared (IR) wavelengths with the X-ray component coming from either a continuation of this synchrotron emission or synchrotron self-Comptonization of the radio/IR emission [10, 11, 12].

In this paper, we present a time series of diffraction-limited, high signal-to-noise ratio images of Sgr A*-IR taken with both the laser guide star (LGS) and natural guide star (NGS) adaptive optics (AO) systems on the Keck II telescope. The LGS AO observations were taken as part of a coordinated campaign, which included observations spanning radio to X-ray wavelengths.

2. Keck Near-IR Adaptive Optics Data

2.1. NIR Observations

On 2005 July 31 (UT), Galactic Center observations in the H- ($\lambda_o = 1.63\mu$m, $\Delta\lambda$=0.30μm), K'- ($\lambda_o = 2.12\mu$m, $\Delta\lambda = 0.35\mu$m), and L'- ($\lambda_o = 3.78\mu$m, $\Delta\lambda$=0.70μm) photometric bandpasses were conducted using the facility near-infrared camera, NIRC2 (K. Matthews 2006, in prep) behind the laser guide star AO system on the W. M. Keck II 10-meter telescope [13, 14]. Observations were made by cycling through the H, K', and L' filters repeatedly for 113 minutes, with a three-filter cycle completed every 3 minutes. Complementary adaptive optics images of the Galactic Center were obtained on 2005 July 16 (UT) using NIRC2 and the AO system in its natural guide star mode [15] by interleaving observations in the L'- and M_s- ($\lambda_o = 4.67\mu$m, $\Delta\lambda = 0.24\mu$m) photometric bandpasses.

2.2. NIR Data Analysis

Identification and characterization of point sources was accomplished using StarFinder, an IDL package developed for astrometry and photometry in crowded stellar fields [16]. StarFinder was first run on an average map made from all the images taken in a night to detect the sources and then run on each individual map with the positions detected in the average map as an input and held fixed, fitting only for source brightness.

Images were photometrically calibrated using the apparent magnitudes of several of the brightest stars in each image [17, 18]. Absolute calibration uncertainties are estimated to be $\sim$4%, 4%, 5%, and 9% at H, K', L', and M_s, respectively. Determination of the uncertainties in the relative photometry of Sgr A*-IR, at all wavelengths, was carried out as in Ghez et al. [19] by calculating the RMS flux density variations between maps for non-variable stars of comparable magnitude. The observed magnitudes were dereddened assuming a visual extinction of 29$\pm$1, an extinction law derived by Moneti et al. (A_H=5.14, $A_{K'}$=3.21, $A_{L'}$=1.56, A_{M_s}=1.46 mag), and flux zero points of 1050, 686, 249, 163 Jy for H, K', L', M_s, respectively [18, 20, 21].

Spectral indices are estimated from near-simultaneous apparent magnitude measurements in pairs of filters. To avoid systematics associated with uncertainties in the extinction law, the spectral index calculations are based on apparent colors that are dereddened using the difference of the apparent colors of S0-2 obtained from the average maps ($H - K = 2.05 \pm 0.03, K - L = 1.25 \pm 0.04, L - M = -0.11 \pm 0.13$) and the intrinsic color of a main sequence B0 star ($H - K = -0.05 \pm 0.08, K - L = -0.16 \pm 0.09, L - M = 0.13 \pm 0.13$; [22, 23, 24]).

Systematic uncertainties from this method include the photometric uncertainty of our measurement of S0-2 and the measurement errors for the colors of B0 stars [22]. The colors of early-type stars are relatively insensitive to spectral type over the small range of uncertainties in the type of S0-2, so there is negligible uncertainty associated with its specific spectral type. When combined quadratically, these errors result in an absolute uncertainty of 0.3, 0.2, and 0.8 for $\alpha_{H-K'}$, $\alpha_{K'-L'}$, and $\alpha_{L'-M_s}$, respectively. The spectral index of several nearby stars were calculated in a similar manner and had the expected stellar indices.

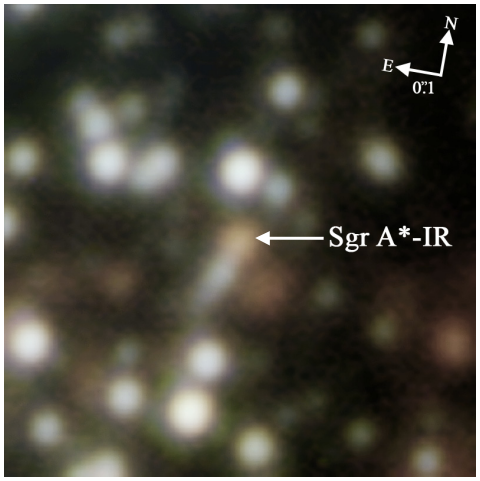

Figure 1. Central $1'' \times 1''$ region of a diffraction-limited false-color image made from the average H (blue), K' (green) and L' (red) images of the Galactic Center taken on July 31 with the LGS AO system. (See the electronic edition for an animation of this image.)

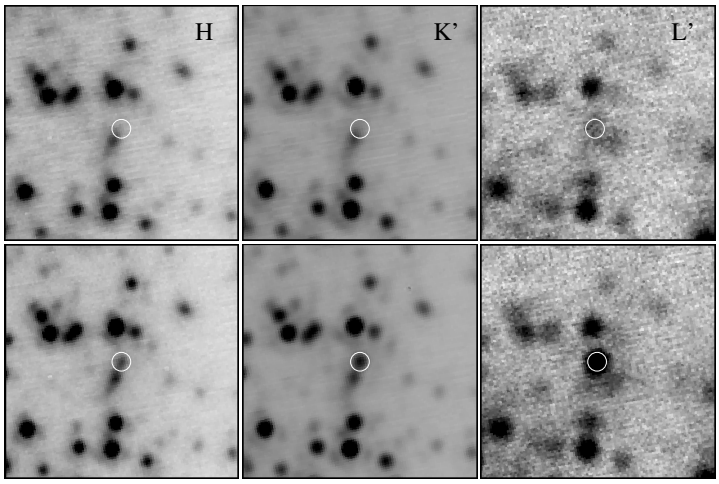

Figure 2. $1'' \times 1''$ images showing Sgr A* (white circle) at its lowest (top) and highest (bottom) states in H, K', and L' on July 31 taken at 08:32 and 07:57 (UT), respectively.

2.3. NIR Results

Figure 1 shows a color composite of the central $1'' \times 1''$ H, K', L' maps from 2005 July 31. From this image, one can see the high density of stars surrounding Sgr A*-IR necessitating that the flux from all stars of comparable brightness to Sgr A*-IR be accounted for. This is especially important when the emission from Sgr A*-IR is at its lowest levels, as shown in the top panel of Figure 2. Even at these faint levels, a point source is detected by StarFinder at the location of Sgr A*-IR with correlation values of >0.7.

Figure 3 displays the dereddened light curves of Sgr A*-IR and comparison stars for the LGS AO H-, K-, and L' observations and the same for the NGS AO L' and M_s observations. During our LGS AO observations on July 31, Sgr A*-IR's light curve shows two clear minima that have values of 2-3 mJy in all three filters and that separate emission that can be associated with three distinct peaks in the IR emission. However, only one maximum is observed in its entirety with peak levels of 9, 12, and 15 mJy in the H, K', and L' filters, respectively (see also the bottom panel of Figure 2). During our NGS AO observations, Sgr A*-IR starts out in a low state similar to the LGS AO observations at 3 and 2 mJy at L' and M_s, respectively, and rises to 7 mJy in both filters by the middle of the observations.

Sgr A*-IR's spectral index appears to be independent of flux density. This is most clearly seen in the spectral index derived from the dereddened K'-L' color (Figure 4). At shorter wavelengths, the spectral indices derived at flux densities below 5 mJy are somewhat bluer. Since this effect is not seen at the longer wavelengths, we attribute this effect to contamination from the underlying stellar population. Since the correlation values of the PSF are still quite high (> 0.7), even at these low emission levels the point source contribution from Sgr A*-IR is still being detected. This background contamination is therefore removed by subtracting off the minimum level observed during the observations, which is taken to be the average level detected during a 10 minute period in the first observed minimum beginning at ∼07:20 (H = 3.2 ± 0.2, K = 2.8 ± 0.1, L' = 3.6 ± 0.2 mJy) for the LGS AO data set and the average of

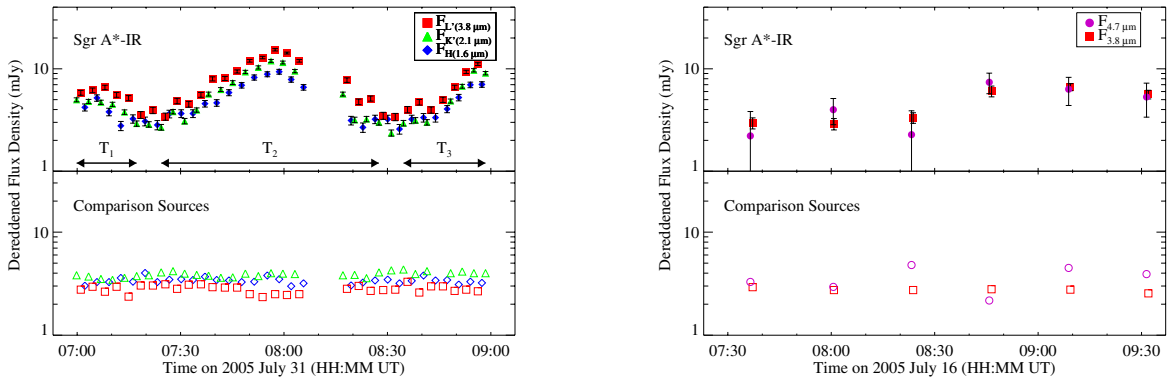

Figure 3. Light curve for Sgr A*-IR and nearby comparison stars of similar brightness at each wavelength for 2005 July 31 (LGS AO; left) and 2005 July 16 (NGS AO; right). The comparison sources are chosen to match the measurements of Sgr A* at its minimum values (S0-37 at H & K', S0-17 at L', and S0-1 at M_s).

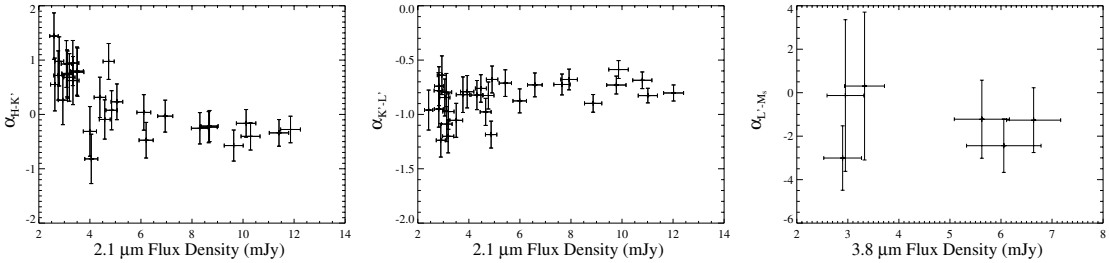

Figure 4. Spectral index ($F_\nu \propto \nu^\alpha$) vs. Sgr A*-IR flux density derived from H-K' (left), K'-L' (center), and L'-M_s(right; not simultaneous with the previous two.) The K'-L' spectral index (middle) shows that the spectral index is independent of flux density.

the first three points for the NGS AO data set (L' = 3.1 ± 0.2, M_s = 2.8 ± 0.9 mJy). With this approach, the spectral indices, as shown in Figure 5, are not only constant with respect to outburst intensity, but also consistent across multiple wavelengths ($\alpha_{H-K'}$ = -1.2 ± (0.4±0.3), $\alpha_{K'-L'}$ = -0.8 ± (0.2±0.2), $\alpha_{L'-M_s}$ = -2.4 ± (0.7±0.8), where the two sources of uncertainty stem from the random photometric errors and the absolute calibration errors, respectively). It should be noted that the K-L' and L'-M_s spectral indices do not change significantly as a result of this subtraction technique, consistent with the assumption that the contaminating background is from the blue stellar population.

Furthermore, as can be seen from Figure 6, we detect no difference in spectral indices within the three separate outburst events. Motivated by this result, we recalculate the spectral index from one pair of K'/L' observations in 2004 [19] using the S0-2 comparison method outlined above and find $\alpha_{K'-L'}$ = -0.8 ± (0.4±0.2) Combining all three 2005 measurements with the 2004 measurement, we infer a near-infrared spectral index for Sgr A*-IR during these observations of α = -0.9 ± 0.2 that is independent of intensity, wavelength, time, or outburst.

Several comments can be made about these results compared to previous results. While photometrically derived spectral indices of Sgr A*-IR are obtained in an inherently different manner than those obtained directly from spectra, they agree within two sigma with OSIRIS K-band (2.02–2.38 μm) spectra obtained at a comparable emission level (i.e. α = -2.6 ± 0.9 when $F_{SgrA*-IR}$ = 6.1 mJy; [25]). Other results, from SINFONI K-band spectra (1.95–2.45 μm),

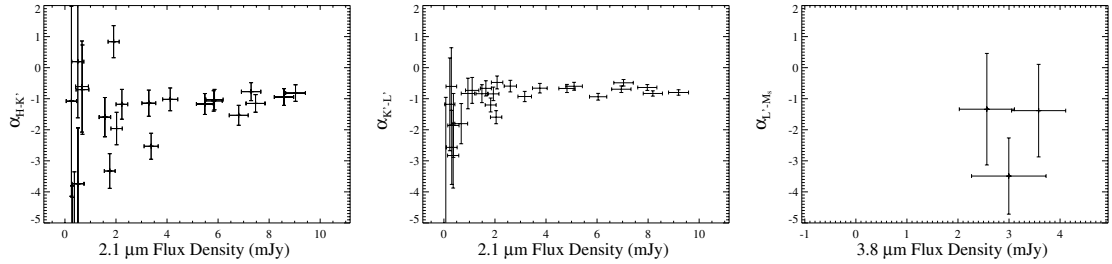

Figure 5. Same as Figure 4 after the background contamination is removed by subtracting the average level of emission during the first minimum for the LGS AO data set and the average of the first three points in the NGS AO data set. The spectral indices across all wavelengths are consistent with each other and have a weighted average of α = -0.9 ± 0.2.

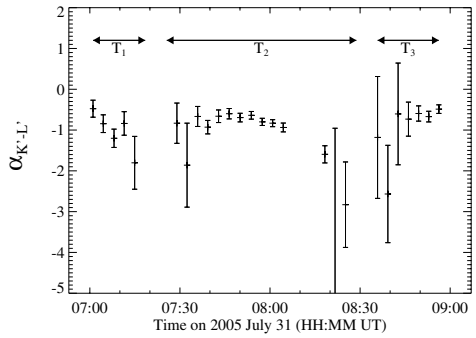

Figure 6. Spectral index derived from K'-L' plotted as a function of time showing no difference in the spectral index within the three separate outburst events (α_{T_1} = -0.9±0.2, α_{T_2} = -0.8±0.3, α_{T_3} = -0.6±0.3).

suggesting a correlation of spectral index with emission intensity [26] are not as discrepant as it may seem. Of the three methods presented by the authors, the 'off state subtraction' method, which most closely resembles the method presented here, shows virtually no correlation down to 2 mJy with $\alpha_{bright\ state} = -0.6 \pm 0.2$. The correlation seen from the other two methods may be explained by the contamination seen in these data below 5 mJy. A local aperture background at K could predominantly sample the contamination from the blue population of surrounding stars and the subtraction of this background would lead to a redder appearance for Sgr A*-IR at low levels (where the background emission becomes comparable to Sgr A*-IR's intrinsic emission.) We therefore believe that the apparent variation in the IR color of Sgr A* in previous experiments arises simply as a consequence of background contamination.

3. Chandra X-ray Data

3.1. ACIS X-ray Observations & Data Analysis

X-ray observations of the Galactic Center were conducted with the *Chandra X-Ray Observatory* [27] using the imaging array of the Advanced CCD Imaging Spectrometer (ACIS-I; [28]) from 2005 July 30 19:44 to 2005 July 31 09:10 (UT). The last two hours of these observations overlapped with the Keck LGS AO observations from the ground. While full details about these observations will be published elsewhere (F. K. Baganoff 2006, in prep), data acquisition and reduction was similar to that reported in [7, 29] (see also [30, 31]).

3.2. X-ray Results

Figures 7 and 8 show the results of the X-ray observations as well as the overlap with ground-based Keck observations. While one moderate-strength outburst is detected, it is not

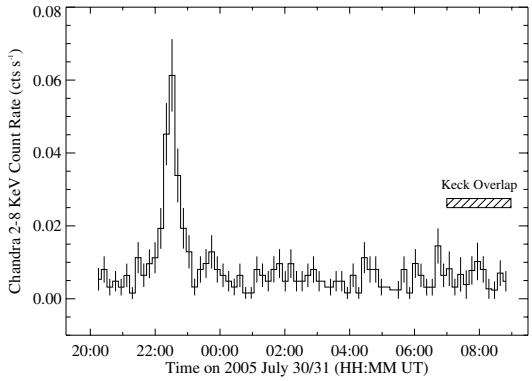

Figure 7. Chandra 2-8 keV light curve of 2005 July 30/31 including the overlap with ground-based Keck observations. The Chandra observations begin on 2005 July 30 20:15:12.0 and end on 2005 July 31 08:49:04.0.

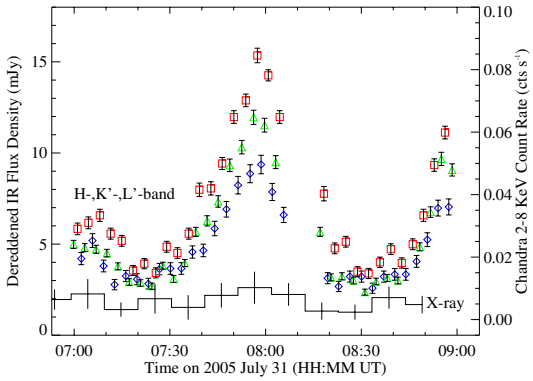

Figure 8. Expanded view of the overlapping X-ray and NIR light curves (See Figure 3 for NIR symbol description). During the entire Keck observations, the X-ray luminosity did not change by more than ∼16%.

simultaneous with the Keck NIR observations. Here we restrict our analysis to the period overlapping the Keck observations. A Bayesian blocks analysis, as described in Eckart et al. [30], was performed on the X-ray light curve without background subtraction. This analysis indicates that Sgr A*'s X-ray light curve is consistent with no variability at the 90% confidence level during the entire remaining period after the outburst. The mean count rate of the background-subtracted light curve from ∼23:00 - 07:00 is 4.29 ± 0.68 cts ks^{-1} corresponding to a 2–8 keV luminosity of 1.8 ± 0.3 × 10^{33} erg s^{-1}. During the Keck overlap, the mean count rate is 4.94 ± 1.54 cts ks^{-1}, which lies within the 90% confidence interval for the period cited above. We therefore adopt an upper limit during the Keck observations of 2.1 × 10^{33} erg s^{-1}. Thus, the X-ray luminosity could not have changed by more than ∼16% during the NIR outburst observed with Keck.

4. Discussion

Comparing the emission presented here with the 12 previously reported 2 μm outburst events, reveals that the peak emission detected on July 31 ranks in the top quartile of all 2 μm outbursts [19, 24, 25, 26, 30, 31, 32]. Furthermore, the low point of infrared emission is comparable to some of the lowest measurements. It is therefore quite notable that, in spite of the wide range of infrared intensities measured, the infrared spectral index is constant. We assume that the infrared probes synchrotron emission from a distribution of relativistic electrons and interpret the lack of variation in the infrared spectral index as an indication that the acceleration mechanism leaves the distribution of the bulk of the electrons responsible for the infrared emission unchanged.

In contrast to the uniformity of the infrared colors, the ratio of infrared to X-ray emission appears to be quite variable. While no elevated X-ray emission was seen during the observations presented here, several previous infrared outbursts (both of higher and lower peak emission levels) have associated X-ray flares [30, 31]. The lack of X-ray variations during our observations indicates that one cannot connect the infrared and X-ray emission to the *same* electrons without invoking a precise tuning of the magnetic field in reaction to a change in the volume of the emitting region such that the X-ray emission could vary substantially while the IR spectral index and intensity remain constant. We therefore suggest that while the acceleration mechanism

leaves the bulk of the electron energy distribution unchanged, it generates a variable high-energy tail. It is this high-energy tail that gives rise to the less frequent X-ray outbursts, which have shown correlated infrared activity in previous studies.

Acknowledgments
Support for this work was provided by NSF grant AST 04-06816 and the NSF Science and Technology Center for Adaptive Optics, managed by UCSC (AST 98-76783). FKB was supported by NASA through Chandra award G05-6093X. The data presented herein were obtained at the W. M. Keck Observatory, which is operated as a scientific partnership among the California Institute of Technology, the University of California and the National Aeronautics and Space Administration. The Observatory was made possible by the generous financial support of the W. M. Keck Foundation.

References

[1] Balick, B., & Brown, R. L. 1974, *ApJ* **194** 265
[2] Ghez, A. M., Salim, S., Hornstein, S. D., Tanner, A., Lu, J. R., Morris, M., Becklin, E. E. and Duchêne, G. 2005a, *ApJ* **620** 744
[3] Schödel, R., Ott, T., Genzel, R., Eckart, A., Mouawad, N. and Alexander, T. 2003 *ApJ* **596** 1015
[4] Falcke, H. 1999, ASP Conf. Ser. 186: The Central Parsecs of the Galaxy, **186** 113
[5] Zhao, J.-H., Young, K. H., Herrnstein, R. M., Ho, P. T. P., Tsutsumi, T., Lo, K. Y., Goss, W. M. and Bower, G. C. 2003 *ApJ* **586** L29
[6] Mauerhan, J. C., Morris, M., Walter, F. and Baganoff, F. K. 2005, *ApJ* **623** L25
[7] Baganoff, F. K. et al. 2001, *Nature* **413** 45
[8] Goldwurm, A., Brion, E., Goldoni, P., Ferrando, P., Daigne, F., Decourchelle, A., Warwick, R. S. and Predehl, P. 2003, *ApJ* **584** 751
[9] Porquet, D., Predehl, P., Aschenbach, B., Grosso, N., Goldwurm, A., Goldoni, P., Warwick, R. S. and Decourchelle, A. 2003, *A&A* **407** L17
[10] Markoff, S., Falcke, H., Yuan, F. and Biermann, P. L. 2001, *A&A* **379** L13
[11] Liu, S. & Melia, F. 2002, *ApJ* **566** L77
[12] Yuan, F., Quataert, E. and Narayan, R. 2004 *ApJ* **606** 894
[13] Wizinowich, P., et al. 2006 *PASP* in press
[14] van Dam, M. A., et al. 2006 *PASP* in press
[15] Wizinowich, P., et al. 2000 *PASP* **112** 315
[16] Diolaiti, E., Bendinelli, O., Bonaccini, D., Close, L. M., Currie, D. G. and Parmeggiani, G. 2000, *Proc. SPIE* **4007** 879
[17] Blum, R. D., Sellgren, K., & Depoy, D. L. 1996, *ApJ* **470** 864
[18] Wright, S. A., et al. 2006, in prep
[19] Ghez, A. M., et al. 2005, *ApJ* **635** 1087
[20] Moneti, A., Stolovy, S., Blommaert, J. A. D. L., Figer, D. F. and Najarro, F. 2001, *A&A* **366** 106
[21] Tokunaga, A. T. and Vacca, W. D. 2005 *PASP* **117** 1459
[22] Ducati, J. R., Bevilacqua, C. M., Rembold, S. B. and Ribeiro, D. 2001, *ApJ* **558** 309
[23] Ghez, A. M., et al. 2003, *ApJ* **586** L127
[24] Eisenhauer, F., et al. 2005, *ApJ* **628** 246
[25] Krabbe, A., Iserlohe, C., Larkin, J. E., Barczys, M., McElwain, M., Weiss, J., Wright, S. A. and Quirrenbach, A. 2006, *ApJ* **642** L145
[26] Gillessen, S., et al. 2006, *ApJ* **640** L163
[27] Weisskopf, M. C., O'dell, S. L. and van Speybroeck, L. P. 1996 *Proc. SPIE* **2805** 2
[28] Garmire, G. P., Bautz, M. W., Ford, P. G., Nousek, J. A., & Ricker, G. R., Jr. 2003 *Proc. SPIE* **4851** 28
[29] Baganoff, F. K., et al. 2003, *ApJ* **591** 891
[30] Eckart, A., et al. 2004, *A&A* **427** 1
[31] Eckart, A., et al. 2006, *A&A* **450** 535
[32] Genzel, R., Schödel, R., Ott, T., Eckart, A., Alexander, T., Lacombe, F., Rouan, D. and Aschenbach, B. 2003, *Nature* **425** 934